Cerrahpaşa Med J 2024; 48(1): 67-73 ORIGINAL ARTICLE

Evaluation of Patients with Liver Biopsy According to the Liver Imaging-Reporting and Data System

Ali Koç[1], Alperen Kayalı[2]

[1]Department of Radiology, Ataköy Imaging Center, İstanbul, Türkiye
[2]Department of Radiology, Hatay Mustafa Kemal University, Faculty of Medicine, Hatay, Türkiye

Cite this article as: Koç A, Kayalı A. Evaluation of patients with liver biopsy according to the liver imaging-reporting and data system. *Cerrahpaşa Med J.* 2024;48(1):67-73.

Abstract

Objective: The aim of the study is to evaluate patients with liver biopsy and histopathological diagnosis according to the Liver Imaging Reporting and Data System (LI-RADS) reporting system and to determine the degree of consistency of the LI-RADS system with histopathological data.

Methods: The histopathological results of a liver biopsy and dynamic imaging were present in 123 cases, which were evaluated according to the LI-RADS radiological reporting system. Major features of LI-RADS and the success of LI-RADS in excluding and predicting hepatocellular cancer (HCC) and non-hepatocellular cancer were evaluated.

Results: The major features of the LI-RADS and Arterial phase hyperenhancement (APHE) were 94.7%, wash-out 84.2%, capsule 89.2%, and threshold growth of 31.6% in HCC. The histopathology of all patients included in the LR-M category also showed non-HCC malignancy. All patients evaluated in the LR-5 group were diagnosed with HCC, except for 1 patient. In that 1 patient who was not diagnosed with HCC, a biopsy may not have been taken from the appropriate area due to the presence of multiple lesions. The histopathological differential diagnosis range of the patients in the LR-3 and LR-4 groups was found to be quite wide.

Conclusion: The abnormal imaging area was characterized in accordance with LI-RADS; its consistency and sensitivity to histopathological data were found to be quite high. Training, dissemination, and implementation of the LI-RADS will increase the consistency and sensitivity of this reporting system. According to our study, we suggest that due to the wide differential diagnosis presence in the LR-3 and LR-4 classes, these cases should be evaluated more carefully, and a multidisciplinary approach would be extremely beneficial.

Keywords: Hepatocellular carcinoma, LIRADS

Introduction

Hepatocellular carcinoma (HCC) is the most common primary liver malignant tumor in the world and the third leading cause of cancer-related deaths.[1,2] It has been observed that overall survival is increased in patients treated with early diagnosis of HCC, such as resection or liver transplantation.[3] The diagnosis of HCC can be made noninvasively by imaging high-risk patients without the need for a percutaneous biopsy.[4-6] Therefore, accurate interpretation and reporting of liver imaging can provide early and appropriate treatment for HCC patients. The Liver Imaging Reporting and Data System (has been designed to meet this need. Free text reports often contain vague statements and may vary according to the experience of the radiologists. This can lead to confusion among clinical teams responsible for the management of HCC or patients at risk of HCC. LI-RADS provides reporting guidelines with an easy diagnosis algorithm to improve radiologists' interpretation, reporting consistency, and clarity.

Although the typical radiological features of hepatocellular carcinoma are known to radiologists, there is no single algorithm that has become widespread and accepted by all radiologists. The Liver Imaging Reporting and Data System (LI-RADS) reporting system, which was first introduced by the American College of Radiology (ACR) in 2011 and was last revised in 2018, aims to fill this gap. Another benefit of LI-RADS is that it improves communication between radiologists and clinicians. According to the LI-RADS diagnostic algorithm, a category (LR-1-LR-5) reflecting the probability of HCC is assigned to liver imaging in a patient at high risk of HCC.[7]

The aim of this study is to categorize patients with biopsy and dynamic examination according to LI-RADS, evaluate them together with pathology findings, and contribute to the use of LI-RADS as a reporting method by increasing its prevalence.

Received: April 12, 2023 **Revision Requested:** July 31, 2023
Last Revision Received: September 27, 2023 **Accepted:** October 17, 2023
Publication Date: March 8, 2024
Corresponding author: Ali Koç, Department of Radiology, Ataköy Imaging Center, İstanbul, Türkiye
e-mail: dr.ali.radyoloji@gmail.com
DOI: 10.5152/cjm.2024.23046

Methods

Data Source and Study Population

The study included 123 patients who underwent liver biopsy for any reason between January 2015 and November 2019 and who had dynamic contrast computed tomography (CT) or dynamic contrast magnetic resonance imaging (MRI) examinations in the radiology department.

The study was approved by Hatay Mustafa Kemal University, Faculty of Medicine (Approval No: 2020/08-32, Date: July 6, 2020). Since it is a retrospective study, participant consent was not required.

Cases with significant artifacts whose radiological imaging did not allow appropriate evaluation were not included in the study. By examining the radiological imaging meticulously, the cases

were placed in LR-1, LR-2, LR-3, LR-4, LR-5, LR-M, and LR-tumor in vein (TIV) classes as a result of the evaluation. The presence of APHE (enhancement in arterial phase), wash-out, capsule, lesion dimensions, and equal growth, if any, were evaluated in each case.

Radiological Imaging Parameters of the Cases in the Study

The MRI examinations of the cases were performed with an Achieva (Philips Medical Systems, Best, The Netherlands) 1.5 Tesla MRI device in the hospital. Precontrast images consisted of DWI images, fat-suppressed T2-weighted and T2-SE images, and mDixon T1-weighted inphase, outphase, fat-suppressed, and water-suppressed images. Postcontrast dynamic images consisted of arterial, portal, and late-phase T1-weighted images and subtraction images in the mDixon series. MRI acquisition protocols FOV: 385-415 mm, matrix: 256 × 256, slice thickness: 4 mm, fat-suppressed T2-weighted axial images [Turbo-spin-echo (TSE) Spectral Presaturation with Inversion Recovery (SPIR), Repetition Time (TR): 1500-2350 ms, Time to Echo (TE): 70 ms, ETL: 24], DWI axial images (DWI) -b1000RT SE EPI B = 0 sec/mm^2, B = 1000 sec/mm^2) values were obtained.

The CT examinations of the cases consisted of arterial and portal phase images obtained using Toshiba Aquilion (64 detectors) devices in the radiology department with KVP: 120, mA: 270-410, 1-5 mm section thickness, FOV: 380-420 mm, matrix: 512 × 512 parameters. Precontrast imaging was not performed in order not to increase the radiation dose received by the patient during the examination.

Contrast agents containing gadolinium (Dotarem, Gadovist, Multihance, Omniscan, and Magnevist) were used in MRI, and iodine-containing contrast agents (Omnipaque, Optiray, and Ultravist) were used in CT for extracellular contrast examinations. Contrast material was administered through the peripheral vein at a rate of 3-5 mL/sec. After the start of contrast agent administration, the late arterial phase is at 35-40 seconds, the portal phase at 60-70 seconds, and the late-phase images were obtained in 3-5 minutes.

Methods Used in Statistical Analysis

Maximum and minimum values, arithmetic mean, standard deviation, and percentage frequencies were calculated in descriptive statistical analysis. The conformity of the data to the normal distribution was evaluated with the Kolmogorov–Smirnov test.

In the comparison of the mean values of 2 independent groups in terms of continuous variables, Student's *t*-test was used in cases of conformity with the normal distribution, and the Mann–Whitney *U*-test was used in the presence of a distribution different from the normal distribution.

Chi-square analysis and Fisher's exact test were used to evaluate 2 independent groups in terms of categorical variables.

All statistical analyses were performed using the SPSS 18.0 program. The significance of the statistical analysis results was evaluated within a 95% CI. *P* values of <.05 were considered significant.

Descriptive Statistical Findings

In our study, we categorized patient lesions according to the current LI-RADS. In the classification of LI-RADS, APHE, the longest diameter of the lesion, wash-out, capsule, and threshold growth criteria are included. The categorization is summarized below in Figure 1.

In our study, 123 cases who underwent liver biopsy for any reason and had dynamic MRI/CT imaging with contrast were included. The gender distribution of the cases was 71/57.7% male and 52/42.3% female. The mean age of all cases was 60.38 ± 14.46 years. The largest diameter of the lesions in the cases was a minimum of 5 mm and a maximum of 203 mm, and the mean of the largest diameters of the lesions was 53.73 mm.

In all of our cases, the number of cases showing the presence of APHE in the selected lesion/imaging area was 29, and the percentage distribution was 23.6%. In all of our cases, the number of lesions that wash out in the selected lesion/imaging area was 20, and the percentage distribution was 16.3%. The number of capsules present in the selected lesion/imaging area in the cases is 48, and the percentile is 39%. The number of threshold enlargements in the cases was 9, which corresponds to 7.3 percent (Table 1).

Evaluation of Cases According to Liver Imaging Reporting and Data System Reporting System and Results

The data of APHE, wash-out, capsule presence, threshold growth, and lesion size, which are the major features of LI-RADS, was analyzed and recorded in MS Office Excel form. The age, gender, and pathology results of the cases were questioned retrospectively through the HIMS system and added to the MS Office Excel file. Categorizing the cases according to LI-RADS according to the latest LI-RADS system of the American College of Radiology.

In the distribution of cases according to LIRADS, the number of LR-1 cases 2, LR-2 cases 21, LR-3 cases 11, LR-4 cases 6, LR-5 cases 17, and LR-M cases is 65, LR – The distribution according to LI-RADS and their percentiles are given in Table 2.

In the cases in the study, the number of histopathologically confirmed HCCs was 19, and the number of non-HCC malignancies was 67. The percentage of cases with HCC was 15.4%.

In the patient group we studied, the mean age of patients with a diagnosis of HCC was higher than that of those with a diagnosis of other malignancies. While the mean age was 70.68 years in the HCC patient population, the mean age was 60.21 years in other non-HCC malignancies. In our study group, although the mean largest tumor diameter of patients with HCC was slightly higher than in patients with other malignancies, the difference was not statistically significant. In our cases, 59% (n = 51) of all our patients with malignancy were male patients, and our HCC rate in male patients was higher than in female patients, and there was a statistically significant difference between the 2 groups. In the chi-square test, the *P*-value was found to be 0.048.

While 94.7% (n = 18) of our patients with HCC confirmed by histopathological diagnosis have APHE, this rate is only 11.9% (n = 8) in non-HCC malignancies. There is a statistically significant difference between the 2 groups. In the chi-square test, the *P*-value was found to be <.001. While there was wash-out in 84.2% (n = 16) of our patients with HCC, this rate is only 3% (n = 3) in non-HCC malignancies. There is a statistically significant difference between the 2 groups. In Fisher's test, the *P*-value was found to be <.001.

Likewise, 84.2% (n = 16) of our patients with HCC had coexistence of APHE and washout, while this rate was only 3% (n = 3) in malignancies other than HCC. There is a statistically significant difference between the 2 groups. In the Fisher test, the *P*-value was found to be <.001.

Capsule is present in 89.5% (n = 17) of cases with a diagnosis of HCC, while this rate is 35.8% in malignancies other than HCC (n = 24). There is a statistically significant difference between the 2 groups. In the chi-square test, the *P*-value was found to be <.001.

While there is threshold growth in 31.6% (n = 6) of HCC cases, this rate is 4.5% (n = 3) in non-HSC malignancies. There is a statistically significant difference between the 2 groups. Fisher's test, *P* = .003, was found.

CT/MRI LI-RADS® v2018 CORE

Untreated observation without pathologic proof in patient at high risk for HCC

- If cannot be categorized due to image degradation or omission → LR-NC
- If definite tumor in vein (TIV) → LR-TIV
- If definitely benign → LR-1
- If probably benign → LR-2
- If probably or definitely malignant but not HCC specific (e.g., if targetoid) → LR-M

Otherwise, use CT/MRI diagnostic table below

- If intermediate probability of malignancy → LR-3
- If probably HCC → LR-4
- If definitely HCC → LR-5

CT/MRI Diagnostic Table

Arterial phase hyperenhancement (APHE)		No APHE		Nonrim APHE		
Observation size (mm)		< 20	≥ 20	< 10	10-19	≥ 20
Count additional major features: • Enhancing "capsule" • Nonperipheral "washout" • Threshold growth	None	LR-3	LR-3	LR-3	LR-3	LR-4
	One	LR-3	LR-4	LR-4	LR-4/LR-5	LR-5
	≥ Two	LR-4	LR-4	LR-4	LR-5	LR-5

LR-4/LR-5 Observations in this cell are categorized based on one additional major feature:
- LR-4 – if enhancing "capsule"
- LR-5 – if nonperipheral "washout" **OR** threshold growth

Figure 1. Computed tomography/magnetic resonance imaging Liver Imaging Reporting and Data System, version 2018 diagnostic algorithm. This material is reprinted without modification with permission from the American College of Radiology (© American College of Radiology; www.acr.org/-/media/ACR/Files/RADS/LI-RADS/LI-RADS-2018-Core.pdf), and pursuant to the Creative Commons BY-NC-ND license and terms contained therein (creativecommons.org/licenses/by-nc-nd/4.0/), including the disclaimer in Section 5. HCC, hepatocellular carcinoma.

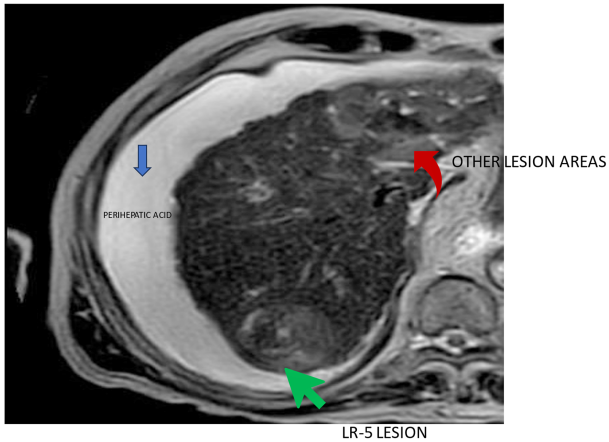

Figure 2. The lesion is observed as hyperintense in the T2-weighted sequence (green arrow indicates lesion).

Two of the histopathologically confirmed HCC patients in our cases were evaluated in the LR-4 category, and 16 HCC patients were categorized as LR-5. The presence of a tumor in the vein was observed in the remaining 1 case and it was added to the LR-TIV category.

Of the 67 cases with histopathologically confirmed non-HCC malignancy, 65 were added to the LR-M category by us, but 2 cases were evaluated in the LR-3 category. These relationships and percentiles are summarized in Table 3.

Since the LR-5 category means a definitive diagnosis of HCC, biopsy is accepted as the gold standard for this category; 16 out of 17 patients included in the LR-5 category were diagnosed with HCC. Two patients evaluated outside the LR-5 category (these 2 patients were evaluated in the LR-4 category) were diagnosed with HCC. For the LR-5 category, LI-RADS had a sensitivity of 88.88% and a specificity of 99.04%. In addition, the positive predictive value of the LR-5 category was 94%, and the negative

Table 1. Frequency and Percentiles of Enhancement in Arterial Phase, Wash-out, Capsule, and Threshold Enlargement in Cases

Major features		n	%
Aphe	Y	29	23,6
	N	94	76,4
Washout	Y	20	16,3
	N	103	83,7
Capsule	Y	48	39
	N	75	61
Threshold growth	Y	9	7,3
	N	114	92,7

N, no; Y, yes.

Table 2. Distribution of Cases According to Liver Imaging Reporting and Data System

LI-RADS Categories	n	%
1	2	1.6
2	21	17.1
3	11	8.9
4	6	4.9
5	17	13.8
M	65	52.8
TIV	1	0.8

Table 3. Distribution of Hepatocellular Carcinoma and Non-hepatocellular Carcinoma malignancies according to Liver Imaging Reporting and Data System Categories

		LI-RADS				
Diagnosis		**3.00**	**4.00**	**5.00**	**M**	**TIV**
HCC	n	0	2	16	0	1
	%	0	10.5	84.2	0	5.3
Non-HCC malignancies	n	2	0	0	65	0
	%	3.0	0	0	97.0	0

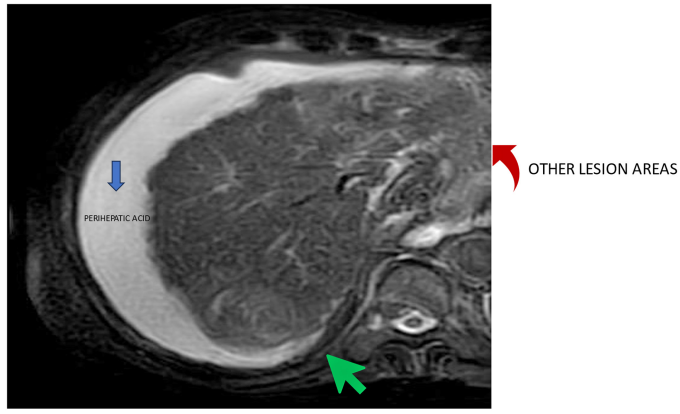

Figure 3. The lesion is observed as hyperintense in fat-suppressed T2-weighted sequence.

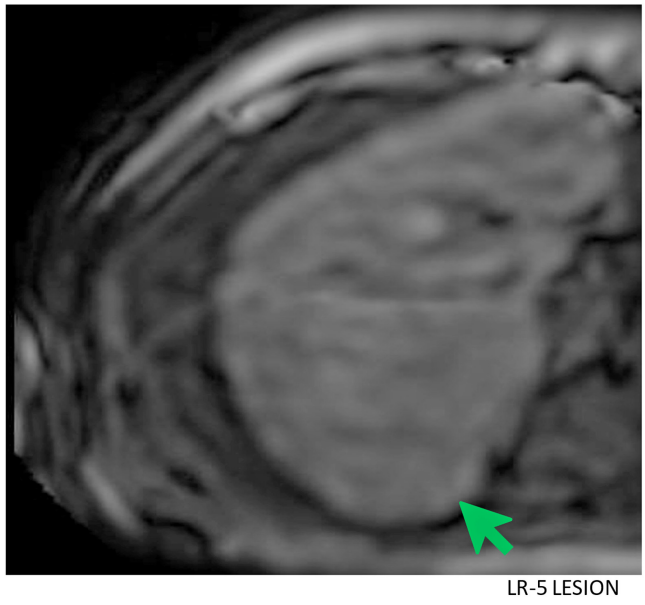

Figure 4. Pre-contrast T1-weighted 3D gradient echo images show the lesion slightly hyperintense (green arrow).

predictive value was 98%. One patient evaluated in the LR-TIV category was excluded in this calculation. If it is also included in the calculation, the sensitivity and specificity will increase even more.

In our research group, although the mean largest tumor diameter of patients with HCC was slightly higher than in patients with other malignancies, the difference was not statistically significant. This

Table 4. Average, Minimum, and Maximum Values of the Largest Tumor Diameters in Hepatocellular Carcinoma and Non-hepatocellular Carcinoma malignancies

Diagnoses	Number of Patient	Minimum	Maximum	Mean (mm)	Standard Deviation
HCC	19	30	145	72.6316	39.26012
Non-HCC Malignancies	67	12	203	56.7313	35.44974

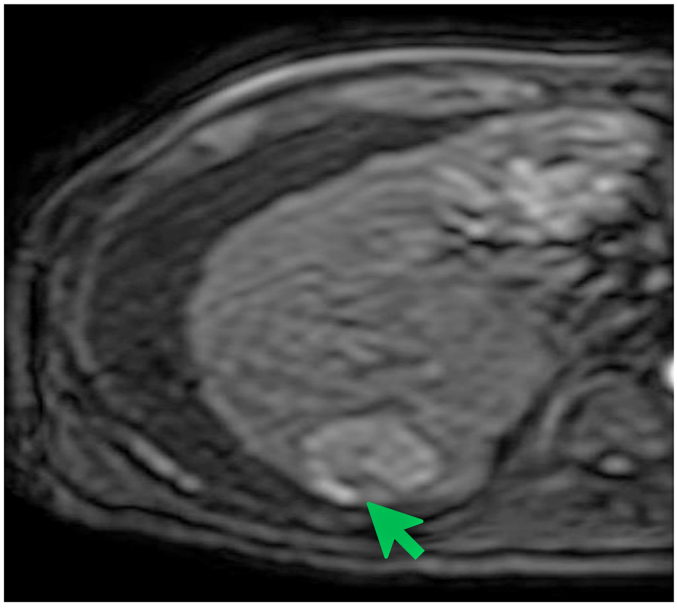

Figure 5. Following administration of a gadolinium-based contrast agent, images of the patient in the late arterial phase.

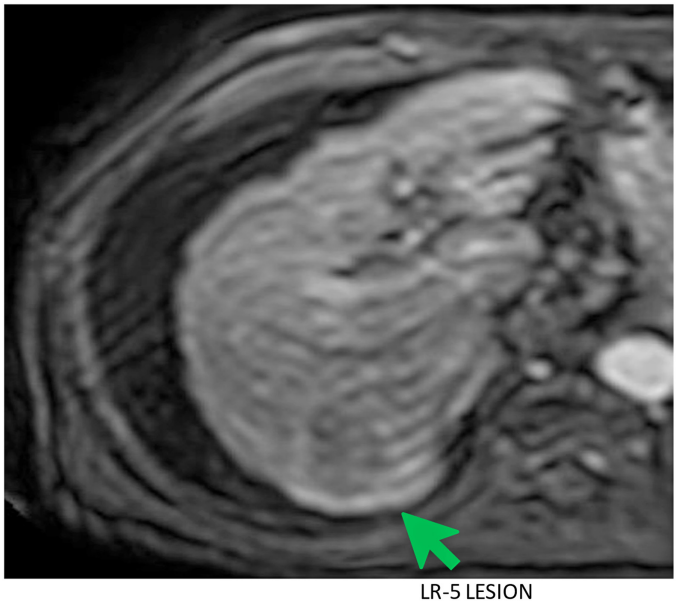

Figure 6. Portal venous phase. The lesion shows wash-out in the portal phase and late venous phase.

is illustrated in Table 4. In the Mann-Whitney *U*-test, the *P*-value was found to be .07.

In our study, the largest diameter of the lesion was 39 mm in 1 patient diagnosed with a cirrhotic nodule, which we categorized as LR-5, and the presence of APHE was present in the lesion. There was also a wash-out and a capsule in the lesion. Since there were multiple lesions in the liver parenchyma in this case, we concluded that the biopsy was not taken from the appropriate place. The pathologist who made the pathological evaluation also approved the biopsy.

Figure 2-7 in order: A case categorized as LR-5 but with benign histopathology

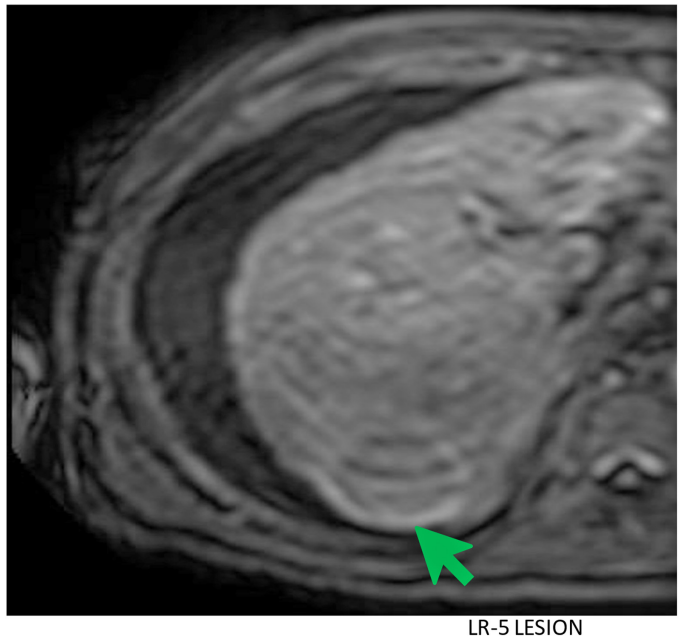

Figure 7. Ring-shaped capsule appearance at the periphery of the lesion in the late venous phase (green arrows) available.

In the patient with multiple lesions in his liver, the histopathological result is a cirrhotic nodule, but we evaluated the lesion in the LR-5 category. The lesion is observed as hyperintense in the T2-weighted sequence (Figure 2) and fat-suppressed T2-weighted sequence (Figure 3). Pre-contrast T1-weighted 3D gradient echo images show the lesion is slightly hyperintense (Figure 4). Following the administration of a gadolinium-based contrast agent, images of the patient in the late arterial phase (Figure 5), portal venous phase (Figure 6), and late venous phase (Figure 7) on T1-weighted 3D gradient echo images. The presence of APHE in the arterial phase of the lesion is remarkable. The lesion shows washout in the portal phase and late venous phase. A ring-shaped capsule appearance at the periphery of the lesion in the late venous phase (arrows) is available. The lesion size was 39 mm.

Discussion

In our study, we evaluated the nodular lesions/abnormal radiological areas detected in patients who underwent liver biopsy according to the latest version of LI-RADS, updated in 2018, and categorized our cases according to this system. We also evaluated the presence of major features in the LI-RADS algorithm. Then, we made a detailed comparison with the histopathological results independent of these findings.

Since our study group consisted of patients who had a biopsy and had lesions / abnormal imaging areas, we tried to target high-risk patients in particular. In this context, we anticipated that we would not be able to reach a sufficient number of patients, as fewer biopsies would be performed in the LR-1, LR-2, and LR-3 risk-free and lower-risk patient populations. Additionally, since the LR-5 patient group, which we referred to as definitive HCC, did not require histopathological confirmation, it was also unknown for us what kind of result we would encounter.

The method of obtaining histopathologically obtained preparations was tru-cut, liver explant, and metastasis excision. Some patients with inadequate sample collection and histopathological

inability to confirm clearly were not included in the study. We also tried to base the safest result on patients with histopathological results of more than 1 liver.

In our study, we evaluated cases without clinical and laboratory information. We considered this method appropriate in order to prevent the clinical and laboratory data on the cases from being a confusing reason for evaluation. However, we think that these data of the cases will have a positive effect on the observers who perform the radiological imaging in the evaluation and decision-making phases.

While 94.7% (n = 18) of our patients with HCC confirmed by histopathological diagnosis had APHE, this rate was found to be only 11.9% in non-HCC malignancies. A statistically significant difference was observed between the 2 groups, and this value was the highest among the major criteria of LI-RADS. The APHE is the most sensitive parameter for HCC among the major criteria.[8-13] This feature was also supported in our study.

While there was APHE and wash-out coexistence in 84.2% (n = 16) of our patients with histopathologically confirmed HCC, this rate is only 3% (n = 3) in non-HCC malignancies. In addition, the presence of wash-out alone was statistically at the same rate. When APHE and wash-out were together, specificity between 81% and 100% and positive predictive values between 87% and 100% were observed in terms of HCC.[11,12,14,15,16] Similar results were found in our study.

Capsules were present in 89.5% (n = 17) of cases with HCC, while this rate was found to be 35.8% (n = 24) in non-HCC malignancies. Although this feature is statistically significant on its own, the third parameter among the LI-RADS major criteria, which increases the diagnostic value the most, together with APHE and wash-out in HCC, was found to be capsule. When we evaluate the coexistence of all 3 (APHE, wash-out, and capsule) in patients with a diagnosis of HCC (n = 19), a rate of 78.9% emerges (n = 15). We can accept this ratio as the sensitivity value for HCC in our research group.

While 31.6% (n = 6) of patients with HCC had threshold enlargement, this rate was 4.5% (n = 3) in non-HCC malignancies. A statistically significant difference was found between the 2 groups. However, since our study was retrospective and our cases were not regularly subjected to active surveillance, as far as we noticed, we think that this data is extremely incomplete.

In our study, we evaluated 65 of our cases in the LR-M category. All of these 65 cases (100%, n = 65) were diagnosed with non-HCC malignancy histopathologically.

In our study, 2 of the 11 patients we evaluated in the LR-3 category were diagnosed with non-HCC malignancy. In this category, 3 patients were diagnosed with confluent fibrosis, 2 with regenerative nodules, 1 with liver adenoma, 2 with confluent necrosis areas, and the remaining 1 with a low-grade dysplastic nodule containing atypical hepatocytes. When we evaluate the LR-3 category in light of these data, we see how wide the range of lesions/abnormal imaging areas is in terms of differential diagnosis and how much knowledge is required for the evaluation of these lesions. In addition, we suggest that these lesions be subject to more active surveillance in order to narrow and clarify the differential diagnosis list and use all the problem-solving aspects of imaging modalities brought about by technological advances.

In our study, there were 6 cases that we categorized as LR-4. Two of them were diagnosed with HCC histopathologically. Of these, 1 case was diagnosed as a dysplastic nodule, and 1 was diagnosed as a cirrhotic large regenerative nodule, 1 was diagnosed as a confluent fibrous. The last remaining LR-4 lesion was also diagnosed a benign vascular lesion.

The histopathological results of all the cases we categorized in the LR-1 and LR-2 groups were also benign.

In light of all this data, we concluded that the LI-RADS system is a secure and consistent data system. In the last version of LI-RADS updated in 2018, in the differentiation of liver lesions from HCC and non-HCC malignancies, we confirmed that it has high sensitivity and specificity values when correct characterization is performed. The widespread use of this system, whose purpose is the use of a common language and standardization in liver lesions, will further increase common knowledge. In addition, the benign pathology results in all LR-1 and LR-2 groups, which did not have a risk for malignancy in our study, reinforced confidence in this system. And for this reason, it will be possible to prevent unnecessary biopsies of these lesions and reduce undesirable situations due to biopsy, thanks to the effective use of the system.

In light of these data, although we think that the LI-RADS system is extremely consistent, we emphasize the importance that it can be further developed by expanding it.

Ethics Committee Approval: Ethics committee approval was obtained at Hatay Mustafa Kemal University, Faculty of Medicine (Approval No: 2020/08-32, Date: July 6, 2020).

Informed Consent: Since it is a retrospective study, participant consent was not required.

Peer-review: Externally peer-reviewed.

Author Contributions: Concept – Ali.K.; Design – Ali.K.; Supervision – Ali.K.; Resource – Ali.K.; Materials – Ali.K.; Data Collection and/or Processing – Ali.K.; Analysis and/or Interpretation – Ali.K., Alperen.K.; Literature Search – Ali.K. Writing – Ali.K.; Critical Review – Alperen.K.

Declaration of Interests: The authors have no conflict of interest to declare.

Funding: The authors declared that this study has received no financial support.

Availability of Data and Material: The datasets used and/or analyzed during the current study are available from the corresponding author on reasonable request.

References

1. Marrero JA, Kulik LM, Sirlin CB, et al. Diagnosis, staging, and management of hepatocellular carcinoma: 2018 practice guidance by the American Association for the Study of Liver Diseases. *Hepatology*. 2018;68(2):723-750. [CrossRef]
2. Serag El MS. Epidemiology of hepatocellular carcinoma. *J Clin Gastroenterol*. 2013;47:S2-S6.
3. Forner A, Reig ME, de Lope CR, Bruix J, eds. Current strategy for staging and treatment: the BCLC update and future prospects. *Semin Liver Dis*. 2010;30(1):61-74. [CrossRef]
4. Chernyak V, Tang A, Flusberg M, et al. LI-RADS® ancillary features on CT and MRI. *Abdom Radiol (NY)*. 2018;43(1):82-100. [CrossRef]
5. Heimbach JK, Kulik LM, Finn RS, et al. AASLD guidelines for the treatment of hepatocellular carcinoma. *Hepatology*. 2018;67(1):358-380. [CrossRef]
6. Tang A, Valasek MA, Sirlin CB. Update on the Liver Imaging Reporting and Data System: what the pathologist needs to know. *Adv Anat Pathol*. 2015;22(5):314-322. [CrossRef]
7. Elsayes KM, Hooker JC, Agrons MM, et al. 2017 version of LI-RADS for CT and MR imaging: an update. *Radiographics*. 2017;37(7):1994-2017.
8. Kim TK, Lee KH, Jang HJ, et al. Analysis of gadobenate dimeglumine–enhanced MR findings for characterizing small (1-2-cm) hepatic

nodules in patients at high risk for hepatocellular carcinoma. *Radiology*. 2011;259(3):730-738. [CrossRef]
9. Lee KH, O'Malley ME, Haider MA, Hanbidge A. Triple-phase MDCT of hepatocellular carcinoma. *AJR Am J Roentgenol*. 2004;182(3):643-649. [CrossRef]
10. Oliver 3rd JH, Baron RL, Federle MP, Rockette Jr HE. Detecting hepatocellular carcinoma: value of unenhanced or arterial phase CT imaging or both used in conjunction with conventional portal venous phase contrast-enhanced CT imaging. *AJR Am J Roentgenol*. 1996;167(1):71-77. [CrossRef]
11. Rimola J, Forner A, Tremosini S, et al. Non-invasive diagnosis of hepatocellular carcinoma ≤ 2 cm in cirrhosis. Diagnostic accuracy assessing fat, capsule and signal intensity at dynamic MRI. *J Hepatol*. 2012;56(6):1317-1323. [CrossRef]
12. Sangiovanni A, Manini MA, Iavarone M, et al. The diagnostic and economic impact of contrast imaging techniques in the diagnosis of small hepatocellular carcinoma in cirrhosis. *Gut*. 2010;59(5):638-644. [CrossRef]
13. Yamashita Y, Mitsuzaki K, Yi T, et al. Small hepatocellular carcinoma in patients with chronic liver damage: prospective comparison of detection with dynamic MR imaging and helical CT of the whole liver. *Radiology*. 1996;200(1):79-84. [CrossRef]
14. Forner A, Vilana R, Ayuso C, et al. Diagnosis of hepatic nodules 20 mm or smaller in cirrhosis: prospective validation of the noninvasive diagnostic criteria for hepatocellular carcinoma. *Hepatology*. 2008;47(1):97-104. [CrossRef]
15. Luca A, Caruso S, Milazzo M, et al. Multidetector-row computed tomography (MDCT) for the diagnosis of hepatocellular carcinoma in cirrhotic candidates for liver transplantation: prevalence of radiological vascular patterns and histological correlation with liver explants. *Eur Radiol*. 2010;20(4):898-907. [CrossRef]
16. Sersté T, Barrau V, Ozenne V, et al. Accuracy and disagreement of computed tomography and magnetic resonance imaging for the diagnosis of small hepatocellular carcinoma and dysplastic nodules: role of biopsy. *Hepatology*. 2012;55(3):800-806. [CrossRef]